



## A study of the vertical scale of halogen chemistry in the Arctic troposphere during Polar Sunrise at Barrow, Alaska

Philip J. Tackett,<sup>1</sup> Aubrey E. Cavender,<sup>1</sup> Adam D. Keil,<sup>1</sup> Paul B. Shepson,<sup>1,2,3</sup> Jan W. Bottenheim,<sup>4</sup> Samuel Morin,<sup>5</sup> John Deary,<sup>4</sup> Alexandra Steffen,<sup>4</sup> and Chris Doerge<sup>6</sup>

Received 12 July 2006; revised 31 October 2006; accepted 21 November 2006; published 7 April 2007.

[1] The vertical extent and impact of halogen chemistry in the Arctic springtime was investigated through balloon-based measurement of several atmospheric chemical components. Various chemical species, including volatile organic compounds (VOCs), ozone, and elemental mercury, that are modified by halogen chemistry were measured from the surface to ~300 m during late March through mid-April 2005 in Barrow, Alaska. It is observed that the halogen chemistry appears to be most active in the lowest 100–200 m of the atmosphere. The Hg vertical concentration profiles are consistent with destruction by chemistry that evolves from a species emitted from the snowpack, most likely Br<sub>2</sub> and BrCl, and the VOC profiles also demonstrate the limited vertical scale of halogen-initiated chemistry taking place above the Arctic snowpack.

**Citation:** Tackett, P. J., A. E. Cavender, A. D. Keil, P. B. Shepson, J. W. Bottenheim, S. Morin, J. Deary, A. Steffen, and C. Doerge (2007), A study of the vertical scale of halogen chemistry in the Arctic troposphere during Polar Sunrise at Barrow, Alaska, *J. Geophys. Res.*, 112, D07306, doi:10.1029/2006JD007785.

### 1. Introduction

[2] It is well known that both ozone (O<sub>3</sub>) and mercury (Hg) are profoundly impacted by chemistry occurring in the lower Arctic atmosphere during springtime. Ozone is an important greenhouse gas [Mickley *et al.*, 2001] and acts as the dominant global source of hydroxyl radicals (OH) through photolysis [Thompson, 1995]. Hydroxyl radicals represent a key component in the oxidative capacity of the atmosphere, and are responsible for the removal of most emitted gases and the destruction of many harmful components, including certain volatile organic compounds (VOCs). However, particularly in polar environments, it is known that halogen atoms are also important oxidants [Jobson *et al.*, 1994]. It has been demonstrated that ozone undergoes a dramatic depletion during the time of polar sunrise [Bottenheim *et al.*, 1986; Oltmans and Komhyr, 1986], and much effort has gone into documenting and quantifying this phenomenon, as well as into determining the chemistry leading to this depletion [Barrie *et al.*, 1988;

Hausmann and Platt, 1994; Tang and McConnell, 1996; Vogt *et al.*, 1996; Impey *et al.*, 1997; Sander *et al.*, 1997; Foster *et al.*, 2001; Bottenheim *et al.*, 2002; Hönninger *et al.*, 2004].

[3] Ozone is believed to be destroyed in the Arctic in a mechanism reminiscent of stratospheric ozone depletion, in which halogen atoms are involved in a chain reaction initiated in the condensed phase as shown in reactions (R1) and (R2) [Barrie *et al.*, 1988; Hausmann and Platt, 1994]:



It has been reported that BrO (produced in reaction (R1)) maximizes during the time of ozone depletion [Hausmann and Platt, 1994; Richter *et al.*, 1998; Hönninger and Platt, 2002]. Barrie *et al.* [1988] first reported the negative correlation between ozone and filterable bromine (sum of particulate Br and gas phase HBr) at Alert (82.5°N, Nunavut, Canada).

[4] In addition to bromine chemistry, chlorine chemistry is also very active at the time of polar sunrise, leading to rapid consumption of VOCs [Kieser *et al.*, 1993; Jobson *et al.*, 1994; Yokouchi *et al.*, 1994; Muthuramu *et al.*, 1994; Ramacher *et al.*, 1997; Ariya *et al.*, 1998]. The observation of rapid alkane consumption cannot be explained by oxidation by Br atoms, as Cl reacts quickly with light hydrocarbons while Br does not [Russell *et al.*, 1988; Jobson *et al.*, 1994]. Research campaigns such as ARCTOC 96 and Polar Sunrise Experiment 1998 have focused on quantifying this chemistry, and results have supported the notion that

<sup>1</sup>Department of Chemistry, Purdue University, West Lafayette, Indiana, USA.

<sup>2</sup>Also at Department of Earth and Atmospheric Sciences, Purdue University, West Lafayette, Indiana, USA.

<sup>3</sup>Also at Purdue Climate Change Research Center, West Lafayette, Indiana, USA.

<sup>4</sup>Science and Technology Branch, Environment Canada, Toronto, Ontario, Canada.

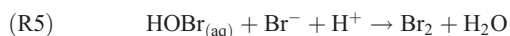
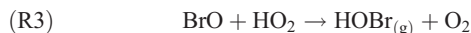
<sup>5</sup>Laboratoire de Glaciologie et Géophysique de l'Environnement, Centre National de la Recherche Scientifique, Université Joseph Fourier, Grenoble, France.

<sup>6</sup>Jonathan Amy Facility for Chemical Instrumentation, Purdue University, West Lafayette, Indiana, USA.

ozone depletion is mainly due to Br-induced oxidation, while particular VOCs are concomitantly depleted primarily by Cl-induced oxidation [Ramacher et al., 1999; Rudolph et al., 1999; Boudries and Bottenheim, 2000].

[5] Recent observations have shown that gaseous elemental mercury (GEM), with a relatively long (6–24 months) atmospheric lifetime and normally slowly varying concentrations, also undergoes rapid destruction during polar sunrise in the Arctic [Schroeder et al., 1998; Lu et al., 2001; Lindberg et al., 2002; Steffen et al., 2005] and Antarctic [Ebinghaus et al., 2002]. The average atmospheric mercury concentration has been reported as 1.7 ng m<sup>-3</sup> in the Northern hemisphere [Slemr et al., 2003]. Although mercury has natural sources, it is also produced anthropogenically via fossil fuel combustion, which, in addition to its long lifetime, makes it difficult to quantify its major local sources [Steffen et al., 2005]. Depletions in Arctic atmospheric mercury concentration have been observed and quantified concurrently with ozone depletion events [Schroeder et al., 1998; Lindberg et al., 2002], suggesting a mechanism that is the same or occurs in concert with that of ozone destruction. The likely GEM oxidants are Br atoms and/or BrO radicals [Lu et al., 2001; Lindberg et al., 2002; Ariya et al., 2004; Sprovieri et al., 2005; Steffen et al., 2005].

[6] Although the destruction of Arctic tropospheric ozone and mercury has been intensely studied, considerable uncertainty lies in the physical source (e.g., ocean, aerosols, or snowpack) of the halogen precursors responsible for this phenomenon. Barrie et al. [1988] proposed that ozone destruction took place in air masses within the stable boundary layer of the Arctic troposphere, which inhibits downward mixing of O<sub>3</sub> from aloft. Significant quantities of photolyzable Br<sub>2</sub> and BrCl have been observed over the saline snowpack surface in Arctic coastal regions [Impey et al., 1997, 1999; Foster et al., 2001]. Upon the bromine-induced destruction of O<sub>3</sub> (reaction (R1)), BrO is produced, followed by reaction with HO<sub>2</sub> to produce HOBr (reaction (R3)), which then reacts with halides in the condensed phase to form Br<sub>2</sub> and BrCl. Fan and Jacob [1992] and Vogt et al. [1996] have proposed that these species are produced via the reaction of HOBr with Br<sup>-</sup> and Cl<sup>-</sup> as shown in reactions (R5) and (R6):



While the Fan and Jacob [1992] mechanism originally envisioned oxidation of the halide ions in aerosols, implying production throughout the boundary layer, Foster et al. [2001] showed that the molecular halogens could be produced by chemistry occurring in the snowpack. This is consistent with the modeling studies of Tang and McConnell

[1996] and Michalowski et al. [2000]. Impey et al. [1997] discussed that their observed springtime Arctic photolyzable bromine and chlorine production rate would rapidly deplete the aerosol phase of halides and thus it was unlikely that aerosols alone could sustain the chemistry. In addition, it has been shown that the sunlit snowpack is highly photochemically active, producing NO<sub>x</sub>, Br<sub>2</sub>, BrCl, HCHO, CH<sub>3</sub>CHO, and HONO, and destroying O<sub>3</sub> [Sumner and Shepson, 1999; Honrath et al., 1999; Peterson and Honrath, 2001; Foster et al., 2001; Zhou et al., 2001; Albert et al., 2002; Guimbaud et al., 2002; Jacobi et al., 2002]. Previous work has suggested that surface O<sub>3</sub> destruction over the snowpack is an inefficient sink mechanism [Langenberg and Schurath, 1999; Wesely and Hicks, 2000; Helmig et al., 2007], yet some work at Summit, Greenland [Peterson and Honrath, 2001; Helmig et al., 2002] and at ALERT2000 [Albert et al., 2002] demonstrated significant photochemically linked surface O<sub>3</sub> loss within the snowpack under stable atmospheric conditions. A one-dimensional modeling study conducted by Lehrer et al. [2004a] comparing two possible sources of halogen atoms (sea salt aerosols and sea ice/snowpack surface) led to the conclusion that halogen atom production from sea salt aerosols is a minor source when compared to surface sources. Thus although it is known that snowpack chemistry can be very active and certainly dramatically impacts chemistry and composition at the surface, it remains uncertain as to what impact it has on chemistry and composition throughout the stable Arctic boundary layer atmosphere.

[7] Ozone concentration vertical profiles have been reported for the lower Arctic troposphere, using data collected from ozonesonde launches during spring 2000 [Bottenheim et al., 2002]. The resultant profiles indicated that a majority of small-scale depletions occur within approximately the lowest 300 m of the troposphere. This was also demonstrated for GEM by Banic et al. [2003]. This observation is consistent with the notion that ozone depletion chemistry may result from halogen precursors that are derived from the snowpack. Previous work near Alert [Mickle et al., 1989; Anlauf et al., 1994; Gong et al., 1997; Hopper et al., 1998] also demonstrated ozone depletion extending from the surface up to 300–400 m. However, this could still be consistent with some halogen activation from sea salt aerosols, as the aerosols and reactants such as HOBr could be confined within the very shallow, stable boundary layer.

[8] Here we report measurements of O<sub>3</sub>, Hg, and VOCs from the surface to ~300 m altitude, in March and April 2005 at Barrow, Alaska. The objective of this study was to gain insights regarding the physical source of the halogen atom precursors and their atmospheric impact through evaluation of the vertical extent of the observed halogen chemistry. We use the ratio of concentrations of methyl ethyl ketone (MEK, CH<sub>3</sub>C(O)C<sub>2</sub>H<sub>5</sub>) to n-butane (C<sub>4</sub>H<sub>10</sub>) as a measure of the local scale oxidative capacity of the atmosphere. Low-level vertical profiles of the concentrations of GEM and VOCs are used to obtain insight into the source of halogen precursors responsible for their destruction, and concurrent vertical profiles of ozone allow for comparison of the mechanism(s) leading to their destruction. Taken together, atmospheric vertical profile data of



**Figure 1.** Map of Arctic region (inset shows NARL sampling location in relation to local geography and prevailing winds), including locations of previous atmospheric research campaigns.

VOCs, mercury, and ozone will provide a closer look into the vertical extent of snowpack and halogen chemistry in the Arctic troposphere.

## 2. Experimental Section

[9] Ozone, gaseous elemental mercury (GEM), and VOC measurements were conducted on the site of the Naval Arctic Research Laboratory (NARL) 4 km northeast of Barrow, Alaska ( $71^{\circ}18'N$ ,  $156^{\circ}47'W$ ), and approximately 5 km southwest of Point Barrow, the northernmost point in the United States, as shown in Figure 1. Measurements were conducted during a period of varying low ozone mole fractions (0 to approx. 20 ppb), from 25 March to 9 April 2005. Partial ozone depletion events were noted during the early portion of the campaign, with a more complete depletion event occurring near the end of the campaign. All measurements were conducted at the same site directly above the snowpack and  $\sim 500$  m from the frozen Chukchi Sea. The prevailing wind direction was generally from the northeast over the Beaufort Sea (i.e., making the site upwind of Barrow, Figure 1), aiding in the prevention of local sources of contamination.

[10] Samples were collected at a vertical range of 0 to 300 m with the aid of a tethered, helium-filled balloon with a lift capacity of approximately 30 kg at 300 m, from which instrument packages were suspended. Varying altitude was achieved with a 12VDC-powered winch, and altitude was determined by monitoring atmospheric pressure at the

sampler in relation to the ground. This information, in addition to ambient temperature, is continuously transmitted to the ground via a 2.4 GHz wireless data logger (Campbell Scientific model CR-205, Logan, Utah) suspended beneath the balloon.

[11] VOC samples were collected through a multiport valve by preconcentration onto Tenax-TA solid sorbent-filled tubes (100 mg, Scientific Instrument Services, Ringoes, New Jersey) mounted in a custom-built autosampler (JAFCl, Purdue University, West Lafayette, Indiana). Samples, acquired at ambient temperature ( $\sim 240$  K), were collected through a short PFA-Teflon inlet at 100 mL/min, controlled by a mass-flow controller, with typical sample volumes of 0.5 L. At this temperature, the breakthrough volume for each measured component was considerably larger ( $>1.1$  L) than the total sample size (0.5 L). Sampling was controlled from the surface using wired communication, and power for the instrument was supplied through a powered tether line. The sample tubes were desorbed at 373 K under He flow, opposite to the direction of sampling (Tekmar AEROTrap 6000, Teledyne Technologies, Mason, Ohio), and preconcentrated at 123 K on a stainless steel loop. Upon desorption, analytes were separated via gas chromatography (Restek RTX-QPlot, 30 m, 0.32 mm ID column) and detected using flame ionization detection (Gow-Mac, Bethlehem, Pennsylvania) within 24 hours of sample collection. Calibrations were performed using gas phase standards created by injection of solutions (in methanol) of liquid phase acetone and MEK (Sigma-Aldrich)

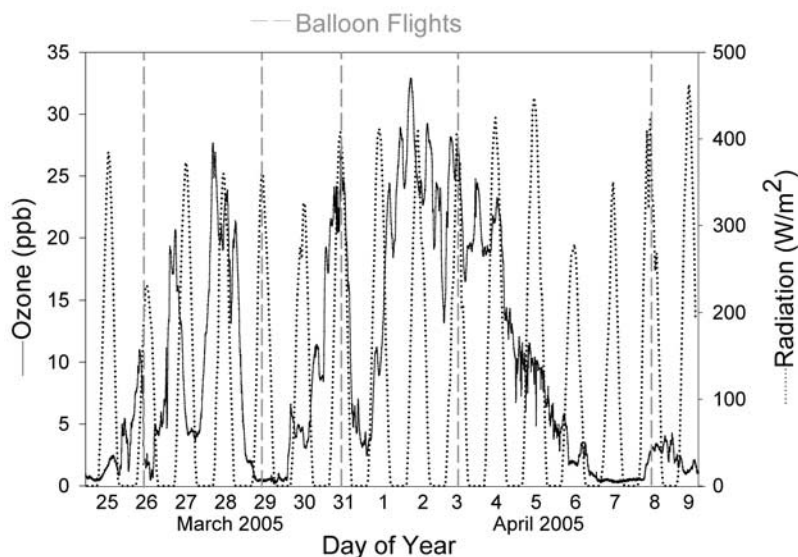


**Figure 2.** Ground-level (15 m asl)  $\text{O}_3$  mole fraction and solar radiation during the measurement campaign (balloon sampler flights labeled in shaded dashed vertical lines), indicating a varying range of  $\text{O}_3$  mole fractions during vertical profile measurements.

and pure gas phase n-butane (Sigma-Aldrich) into a balance of air (UHP grade, Airgas) in PFA Teflon bags. Blanks were collected using sample tubes mounted within the same path as the samples but not containing a sample volume. Instrument calibration precision was  $\pm 3\%$ , and total uncertainty in the measurement technique was approximately  $\pm 10\%$ . Limits of detection (based on three times the standard deviation of the blanks) were approximately 400 ppt for acetone, 150 ppt for methyl ethyl ketone, and 40 ppt for n-butane. All measured VOC concentrations for the vertical profile data were above the limit of detection, with the exception of the highest altitude collection point for MEK measured on 8 April, which had a signal-to-noise ratio of approximately 2.

[12] An explicit zero-dimensional photochemical model was employed to demonstrate the impact of chlorine-induced oxidation of n-butane. The model is similar to that used by *Grannas et al.* [2002]. Gas phase halogen chemistry was integrated into the model, using fluxes of  $\text{Cl}_2$  and  $\text{BrCl}$  to produce  $\text{Cl}$  and  $\text{Br}$  atom concentrations consistent with measured values [Keil and Shepson, 2006]. Available data specific to the Barrow, Alaska sampling site were used for many parameters, including temperature, photolysis rate constants, and ozone and n-butane concentrations. Formaldehyde ( $\text{HCHO}$ ) was fixed at  $6 \times 10^9$  molecules  $\text{cm}^{-3}$  [Grannas et al., 2002], and  $\text{NO}_x$  was generated through fluxes of  $\text{HONO}$  and  $\text{NO}$  depending on solar radiation specific to the sampling location.

[13] GEM measurements were conducted by continuously drawing ambient air through a PFA-Teflon inlet line that was connected from the balloon to a vapor phase mercury analyzer (Tekran Inc. Model 2537A, Toronto, Canada) located in a small hut on the surface. Full descriptions and operating parameters of the Tekran have been published elsewhere [Lindberg et al., 2000]. The analyzer operates by preconcentrating GEM onto traps consisting of gold beads prior to thermal desorption into a cold vapor atomic

fluorescence spectrometer. A Teflon filter (47 mm diameter,  $0.2 \mu\text{m}$  pore size) was installed on the sample inlet to prevent the admission of particles likely to contribute significantly to particulate mercury. It is likely that particles with aerodynamic diameters smaller than  $0.2 \mu\text{m}$  contribute to the measured GEM.

[14] The overall length of the inlet line restricted the vertical range of GEM measurements to 120 m, except for the 8 April GEM measurement, in which a 30 m inlet line was used. For all vertical profiles, the entire sample line was used for measurements at all altitudes, yielding a consistent maximum sample residence time of approximately 1 min. The instrument was allowed to sample at each altitude for sufficient time to allow the line to flush and continuously collect multiple measurements to assess precision. For altitudes in which three or more continuous GEM measurements were made, the 1 s precision is presented as an error bar. GEM measurements not represented with an error bar are displayed as the mean of two measurements at the associated altitude, with a  $4(\pm 6)\%$  average deviation from the mean. The average collection time for a single GEM measurement was on the order of 5 min. Ozone vertical profile data were collected by suspending a self-contained, 12VDC-powered spectrophotometer (2B Technologies, Golden, CO) in a temperature-controlled ( $12^\circ\text{C}$ ) vessel beneath the balloon. The ozone instrument has a limit of detection of  $1.5(\pm 1)$  parts per billion (ppb), and was calibrated in the field against a TEI Model 165 ozone generator that was itself standardized against a NIST transfer standard.

### 3. Results and Discussion

#### 3.1. Ozone and Mercury

[15] In Figure 2 we present the ground-level  $\text{O}_3$  measured at the NOAA Global Monitoring Division laboratory

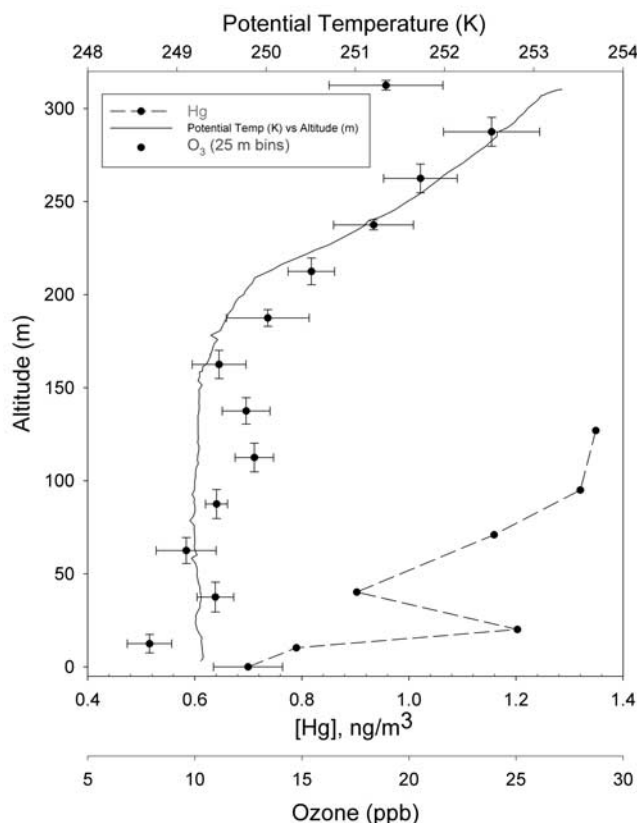


**Figure 3.** Vertical concentration profiles of O<sub>3</sub> (binned), GEM, and potential temperature for 31 March 2005 from NARL runway.

(71°15'15"N, 156°30'27"W) during the balloon flights. Surface O<sub>3</sub> mole fractions ranged from ~1 to ~30 parts per billion (ppb), and the five flights covered a range of partially depleted conditions.

[16] Vertical concentration profile data obtained during the flight on 31 March 2005, including ozone, GEM, and potential temperature, are shown in Figure 3. The ozone data indicate the existence of a partial ozone depletion event, with a ground-level O<sub>3</sub> mole fraction of approximately 7 to 9 ppb, increasing to greater than 20 ppb at a height of 300 m. The shape of the potential temperature data (solid line, Figure 3) indicates the relative vertical stability of the atmosphere during the time of the balloon flight, inhibiting downward mixing of O<sub>3</sub> from aloft. Such a stable boundary layer was the typical condition for all flights. The data in Figure 3 show that O<sub>3</sub> and Hg were depleted in the neutral layer that exists from the surface to 200 m. However, the overall shapes of the ozone and mercury profiles are distinctly different, with Hg showing a steeper gradient, implying relatively faster depletion near the surface. The available 1s error bars (Figure 3) suggest that this difference in the profiles for ozone and GEM is real.

[17] *Schroeder et al.* [1998] were the first to observe that the concentration of GEM at Alert frequently drops below 1 ng m<sup>-3</sup> during the 3-month period following Polar Sunrise. Similar observations have been reported for other Arctic stations such as Barrow [*Lindberg et al.*, 2002], Ny Ålesund [*Berg et al.*, 2003], and in Antarctica [*Ebinghaus*

*et al.*, 2002]. Consistent with these reports, we observed that ground-level GEM concentrations frequently dropped to as low as 0.6 ng m<sup>-3</sup> at the surface (see Figure 4, which shows the GEM data for all our flights), although *Lindberg et al.* [2002] have reported depletion events in Barrow with GEM concentrations below 0.5 ng m<sup>-3</sup> (consistent with the 8 April profile).

[18] In Figure 4 we plot GEM data for each balloon launch, including the measured surface O<sub>3</sub> mole fractions at the time of the launch. Also shown for reference is the average Northern hemisphere ambient GEM concentration [*Slemr et al.*, 2003]. In all cases, GEM appears to be depleted at the surface relative to the seasonal average in the Arctic, with a majority of the depletion being confined to the lowest ~60 to 100 m above the surface. This appears consistent with the work of *Banic et al.* [2003], who reported GEM concentration profiles on a larger vertical scale (from 0.1 to 7 km) using aircraft-based instrumentation, and a similar low-level depletion was noted below 1 km.

[19] There have been several studies of the potential chemical reactants responsible for Arctic Hg<sup>0</sup> depletion [*Lindberg et al.*, 2002; *Ariya et al.*, 2004; *Raofie and Ariya*, 2004; *Calvert and Lindberg*, 2005; *Donohoue et al.*, 2006; A. L. Sumner et al., Gaseous elemental mercury oxidation under conditions of relevance to the atmosphere, submitted to *Environmental Science and Technology*, 2006]. The primary reaction leading to GEM depletion most likely

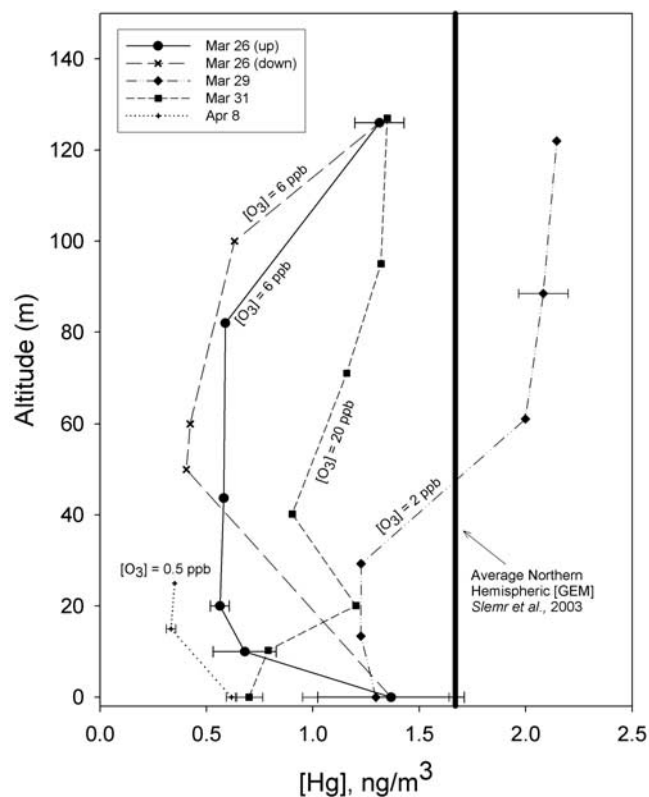
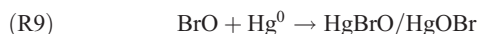
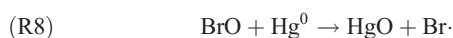


**Figure 4.** GEM vertical concentration profiles, ground-level ozone mole fraction (NOAA Global Monitoring Division), and published Northern Hemispheric ambient Hg<sup>0</sup> concentration [*Slemr et al.*, 2003].

involves oxidation primarily by Br, and to a lesser extent by BrO (reactions (R7)–(R10)) [Ariya *et al.*, 2004]:



While recent publications have implied that the oxidation of GEM by BrO is slightly endothermic [Tossell, 2003], suggesting that the primary pathway for GEM oxidation occurs with Br, the rate constant measurements imply this is not the case. The work of Raofie and Ariya [2004] showed that all of HgO, HgOBr/HgBrO, and HgBr were observed for the reaction of BrO and Hg<sup>0</sup>, but some of these products could have been heterogeneously produced. The rate constants for the oxidation of GEM by Br and BrO have been measured by several groups. For the Br atom reaction, the measured rate constant ranges from  $1.1 \times 10^{-12}$  [Goodsite *et al.*, 2004] to  $6.3 \times 10^{-13} \text{ cm}^3 \text{ molecule}^{-1} \text{ s}^{-1}$  [Donohoue *et al.*, 2006]. For the BrO reaction, the rate constant has been reported within a range of  $1 \times 10^{-13}$  to  $1 \times 10^{-15} \text{ cm}^3 \text{ molecule}^{-1} \text{ s}^{-1}$  [Raofie and Ariya, 2003]. For this analysis, we will calculate the first-order rates of reaction using the upper and lower limits of the rate constant for both reactions.

[20] Given estimated/measured Br and BrO concentrations during ozone depletion events of  $\sim 1 \times 10^7$  [Jobson *et al.*, 1994] and  $5 \times 10^8 \text{ molecules cm}^{-3}$  [Hönninger and Platt, 2002], this leads to an estimated first-order rate for Hg reaction between  $1.1 \times 10^{-5}$  and  $6.3 \times 10^{-6}$  for Br, and between  $5 \times 10^{-5}$  and  $5 \times 10^{-7}$  for BrO. Although the rate constants are both quite uncertain at this point, it appears that both Br and BrO may be important reactants. Assuming that both reactions occur, this leads to a Hg lifetime within a range of approximately 4.6 and 41 hours during O<sub>3</sub> depletion events, which is considerably shorter than the lifetime of O<sub>3</sub>. This and the possibility of different uptake mechanisms in the snowpack may help explain the distinctly different profiles for O<sub>3</sub> and Hg, as shown in Figure 3.

[21] Although not measured in this particular campaign, the low early polar springtime O<sub>3</sub> concentrations suggest that BrO is present at relatively high concentrations in the atmosphere, on the basis of the reported negative correlation of O<sub>3</sub> with BrO [Hausmann and Platt, 1994; Hönninger and Platt, 2002]. It has also been shown that elevated levels of reactive gaseous mercury (RGM), produced from oxidation of GEM, have been measured concomitant with increased levels of BrO during a field campaign in Barrow [Lindberg *et al.*, 2002]. Given the stable atmospheric conditions during the measurement period (demonstrated by the potential temperature plots in Figures 3 and 7), the demonstrated vertical profiles suggest that surface-level oxidation appears to be prevalent, symptomatic of the precursors to this oxidation mechanism coming from the snowpack. This

is consistent with the hypothesis that the reactant is most likely Br and/or BrO, and that the precursor to these reactants is Br<sub>2</sub> and/or BrCl derived from the snowpack [Simpson *et al.*, 2005]. Simpson *et al.* [2005] reported that snow near the Barrow coastline is depleted of bromide (while it is enhanced further inland) as compared to sea-salt composition, consistent with heterogeneous chemistry within the snowpack that produces photolabile Br<sub>2</sub> and BrCl from the reaction of halides with HOBr (reactions (R5) and (R6)). In this scenario, dry-deposited sea salt and HOBr/HBr is reprocessed by HOBr, resulting in the release of Br<sub>2</sub> and BrCl from the snowpack [Foster *et al.*, 2001; Simpson *et al.*, 2005].

[22] As mentioned above, the faster relative rate of GEM destruction may help explain the steeper GEM profile relative to that for ozone, given similar rates of reactant diffusion from aloft. However, this seems somewhat inconsistent, as ozone eventually becomes completely depleted, while GEM never exhibits total destruction in the boundary layer. This suggests that the near-surface portion of the GEM profile may be impacted by photoreduction of RGM within the snowpack, essentially providing a source of GEM during conditions when both ozone and mercury destruction are occurring. Given the fast relative rates of destruction, the possible existence of a surface source of GEM is unlikely to have a substantial impact beyond the absence of total near-surface GEM destruction.

[23] Previously published research on atmospheric mercury in high latitudes has demonstrated that upon halogen-induced oxidation, GEM is converted to more water-soluble products, known as reactive gaseous mercury (RGM) and particulate phase Hg oxidation products, that undergo dry deposition into the snowpack [Lu *et al.*, 2001; Dommergue *et al.*, 2003]. Photoinduced reduction of Hg(II) to volatile GEM has been demonstrated through the measurement of increased GEM concentration above snowpack samples upon irradiation [Lalonde *et al.*, 2002]. Elevated GEM concentrations have also been measured directly above the snowpack at Alert, likely because of solar irradiation of RGM on the surface [Steffen *et al.*, 2002]. These observations are consistent with the notable increase in ground-level GEM concentration in the profiles for 26 March (Figure 4). However, the light intensity (Figure 2) is lower for the 26 March flight compared with the others. There are, of course, multiple variables that impact the profile shape, since the gas phase destruction rate is light-dependent, while the emission of GEM from sunlit snowpack must be at least partially dependent on recent rates of deposition of RGM and particulate phase Hg.

[24] The other Hg profiles imply consumption by a species emitted from the snowpack, with a rate that decreases rapidly with altitude. As discussed by Lehrer *et al.* [2004a], the Br<sub>2</sub> concentration (and thus [Br]) is expected to decrease rapidly with altitude. We can calculate its effective mixing height ( $Z^*$ ) via the method of Guimbaud *et al.* [2002], given a value for  $J_{\text{Br}_2}$  of  $2.2 \times 10^{-2} \text{ s}^{-1}$  [Madronich and Flocke, 1998] (or  $\tau_{\text{Br}_2}$  is  $\sim 45 \text{ s}$ , during midday early April at Barrow, Alaska), as shown in equation (1):

$$Z^* = \sqrt{K_c \tau} \quad (1)$$

**Table 1.** Rate Constants and Oxidant/Reactant Concentrations Used in the Calculation of BrO<sub>x</sub> Lifetime at 245 K<sup>a</sup>

Reaction	Rate Constant, cm <sup>3</sup> molecule <sup>-1</sup> s <sup>-1</sup> (Reference)	[Oxidant], molecules cm <sup>-3</sup>	[Reactant], molecules cm <sup>-3</sup> (Reference)
Br + HCHO ( <i>k</i> <sub>11</sub> )	6.63 × 10 <sup>-13</sup> (1)	1.0 × 10 <sup>7</sup>	6.2 × 10 <sup>9</sup> (4)
Br + CH <sub>3</sub> CHO ( <i>k</i> <sub>12</sub> )	2.99 × 10 <sup>-12</sup> (1)	1.0 × 10 <sup>7</sup>	3.1 × 10 <sup>9</sup> (4)
BrO + NO <sub>2</sub> ( <i>k</i> <sub>13</sub> )	1.22 × 10 <sup>-11</sup> (2)	7.5 × 10 <sup>8</sup>	2.5 × 10 <sup>8</sup> (5)
BrO + HO <sub>2</sub> ( <i>k</i> <sub>3</sub> )	4.74 × 10 <sup>-11</sup> (3)	7.5 × 10 <sup>8</sup>	1.25 × 10 <sup>8</sup> (5)

<sup>a</sup>References: 1, *Atkinson et al.* [2001]; 2, *DeMore et al.* [1997]; 3, *Sander and Crutzen* [1996]; 4, *Michalowski et al.* [2000]; 5, *Honrath and Jaffe* [1992].

Using a range of surface-level turbulent eddy diffusivities ( $K_c$ ) from 95 [*Guimbaud et al.*, 2002] to 700 cm<sup>2</sup> s<sup>-1</sup> [*Lehrer et al.*, 2004b], the effective mixing height for Br<sub>2</sub> is approximately 1 to 2 m. These  $K_c$  values are consistent with the measured Arctic surface layer eddy diffusivities (~100–400 cm<sup>2</sup> s<sup>-1</sup>) reported by *Honrath et al.* [2002] and *Jacobi et al.* [2002]. Since data were collected throughout the day,  $J$  values can vary from a minimum of ~1.2 × 10<sup>-2</sup> s<sup>-1</sup> to the maximum reported above, which leads to a very narrow theoretical range of vertical distances (from approximately 0.5 to 2.5 m) over which Br<sub>2</sub> will be converted to Br. For Hg, assuming  $\tau_{\text{Hg}}$  in the surface layer of ~18 hours, we obtain  $Z^* \sim 10$ –20 m. This is not inconsistent with the bottom of the 26 March GEM profiles, in which Hg is relatively (and statistically significantly) elevated in the lowest ~20 m.

[25] Upon photolysis, Br rapidly interconverts between Br and BrO in the presence of O<sub>3</sub>, and both Br and BrO (referred to as BrO<sub>x</sub>) can oxidize GEM. Given a typical, average daytime [Br] of 1.0 × 10<sup>7</sup> molecules cm<sup>-3</sup> [*Keil and Shepson*, 2006] and [BrO] of 7.5 × 10<sup>8</sup> molecules cm<sup>-3</sup> [*Hönninger and Platt*, 2002], the lifetime of BrO<sub>x</sub> is estimated to be ~110 s on the basis of the following reactions that terminate BrO<sub>x</sub> (reactions (R3) and (R11)–(R13)) [*Shepson et al.*, 1996]. Initial concentrations of reactants and rate constants are given in Table 1.



On the basis of an estimated BrO<sub>x</sub> lifetime of 110 s, the vertical distribution of BrO<sub>x</sub> can be estimated to extend an additional ~1–3 m above the snowpack.

[26] However, it should be noted that HOBr produced in termination reaction (R3) undergoes photolysis on a time-scale of about 0.5 hours. This corresponds to an additional ~4 m by which Br-atom precursors (via HOBr photolysis) extend in the vertical direction. The contribution to bromine atom production, however, is considerably less for HOBr photolysis than from Br<sub>2</sub> photolysis given expected concentrations of Br<sub>2</sub> and HOBr. Given a measured ratio [HOBr]/[Br<sub>2</sub>] on the order of 10 [*Impey et al.*, 1999], the

impact of HOBr photolysis on Br-atom production can be calculated (equation (2)):

$$\frac{d[\text{Br}]_{\text{from HOBr}}}{d[\text{Br}]_{\text{from Br}_2}} = \frac{J_{\text{HOBr}}[\text{HOBr}]}{2 \cdot J_{\text{Br}_2}[\text{Br}_2]} \quad (2)$$

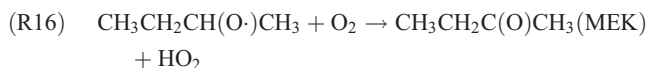
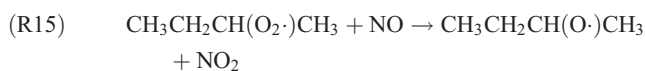
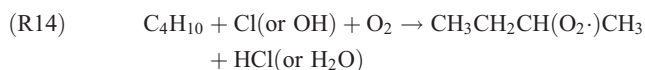
Given a ratio of  $J_{\text{HOBr}}/J_{\text{Br}_2}$  of ~0.05, the relative contribution of the production of Br atoms from Br<sub>2</sub> is estimated to be ~4 times greater than from HOBr photolysis.

[27] In summary, if the reactants for GEM are Br and/or BrO, and the precursors to these are produced in the snowpack, then all the depletion chemistry would occur in the lowest ~10 m of the boundary layer. In contrast, the demonstrated depleted region is from ~0 to 50–100 m. If the precursors all derive from the surface, then this suggests that the depleted layer expands because of diffusion of reactants such as Hg, O<sub>3</sub>, and VOCs from aloft into the surface layer in which the chemistry occurs, likely because of light turbulent mixing within the stable boundary layer. Thus, for many species, their atmospheric lifetime in the Arctic will be determined in part by the timescale for diffusion into the surface layer.

### 3.2. Volatile Organic Compounds (VOCs)

[28] In the same fashion that Br chemistry destroys mercury, Cl chemistry also rapidly destroys VOCs with relative rates that depend on Cl and VOC rate constants. These relative rates can be used to identify the nature of the reaction partner [*Jobson et al.*, 1994]. Arctic seasonal trends in light hydrocarbons have been shown to demonstrate changes in OH concentration [*Jobson et al.*, 1999; *Swanson et al.*, 2002], but VOC destruction continues (albeit at a slower rate) during the winter, when OH concentrations are low [*Spivakovsky et al.*, 1990]. In addition to oxidation by OH, halogen atoms such as Cl and Br are known to play a role in the destruction of these species in the lower Arctic troposphere [*Pszenny et al.*, 1993; *Jobson et al.*, 1994; *Keil and Shepson*, 2006].

[29] When n-butane is oxidized by OH or Cl (assuming H-abstraction occurs on C<sub>2</sub> or C<sub>3</sub>), methyl ethyl ketone (MEK) is produced as shown:



The [MEK]/[butane] ratio can be calculated via equation (3) on the basis of the known rate constants (Table 2), product yields, and estimated ambient radical concentrations,

**Table 2.** Rate Constants and OH/Cl Concentrations Used in Calculation of Theoretical [MEK]/[Butane] Ratio (Equation (3))<sup>a</sup>

Reaction	Rate Constant, cm <sup>3</sup> molecule <sup>-1</sup> s <sup>-1</sup> (Reference)	[Oxidant], molecules cm <sup>-3</sup> (Reference)
OH + n-butane	1.5 × 10 <sup>-12</sup> (1)	1.0 × 10 <sup>6</sup> (5)
OH + MEK	1.2 × 10 <sup>-12</sup> (2)	1.0 × 10 <sup>6</sup> (5)
Cl + n-butane	2.2 × 10 <sup>-10</sup> (3)	7.5 × 10 <sup>4</sup> (6)
Cl + MEK	2.7 × 10 <sup>-11</sup> (4)	7.5 × 10 <sup>4</sup> (6)

<sup>a</sup>References: 1, *DeMore and Bayes* [1999]; 2, *Atkinson et al.* [2001]; 3, *Tyndall et al.* [1997]; 4, *Cuevas et al.* [2004]; 5, *Grannas et al.* [2002]; 6, *Boudries and Bottenheim* [2000]. Concentrations are midday, Arctic springtime maxima and rate constants are for T = 240 K except *Tyndall et al.* [1997], which is at T = 298 K.

assuming production and loss via the following consecutive reactions.



$$\frac{[\text{MEK}]}{[n - \text{butane}]} = \frac{\alpha_x \cdot k_{18} \cdot (1 - e^{-(k_{18} - k_{19}) \cdot [\text{oxidant}] \cdot t})}{(k_{19} - k_{18})} \quad (3)$$

This calculation can be used to estimate the relative impacts of Cl and OH on the [MEK]/[butane] ratio given estimated [OH] and [Cl], and the MEK yields,  $\alpha_x$ . Using the rate constants and oxidizer concentrations (from measurements and models for Alert) given in Table 2,  $k_{OH}[\text{OH}] = 1.5 \times 10^{-6} \text{ s}^{-1}$  for the first step in the two-reaction sequence (the oxidation of n-butane) and  $k_{OH}[\text{OH}] = 1.2 \times 10^{-6} \text{ s}^{-1}$  for the second step in the sequence (MEK product oxidation). The yield values,  $\alpha_x$ , for x = Cl and OH are 0.71 and 0.89, respectively.

[30] Equation (3) then yields a [MEK]/[butane] ratio of approximately 0.12 after 24 hours if the oxidizer is OH, but

approximately 2.0 after 24 hours when Cl is the oxidizer. Thus we expect that under Arctic ozone depletion conditions, this ratio is impacted to a greater extent by Cl atom chemistry, and thus is indicative of the magnitude of the extent of Cl atom chemistry for such conditions.

[31] The ratio of [MEK] to [n-butane] can be used as a measure of the local scale oxidation power of the atmosphere. Although both OH and Cl are capable of oxidizing butane to produce MEK (as shown in reactions (R14)–(R16)), the analysis described above indicates that it is more sensitive to Cl-atom chemistry. It should also be noted that the rate of Br-induced alkane oxidation is several orders of magnitude slower than for both Cl and OH, and likely to be of little effect in the destruction of Arctic n-butane. To further illustrate the impact of halogen chemistry on VOC oxidation, a zero-dimensional photochemical model was employed (as described in section 2). This model includes much of the known oxidation chemistry that occurs in the Arctic for alkanes up to four carbons, including a detailed oxidation scheme for n-butane. The results of this model, in terms of the impacts on the [MEK]/[n-butane] ratio, are shown in Figure 5.

[32] Figure 5 demonstrates the simulated time-dependent radical-induced oxidation of n-butane, and shows how the [MEK]/[n-butane] ratio changes with time, with OH-only chemistry, and with the simulated halogen atom chemistry. Figure 5 indicates the daytime average concentrations of the radicals, at the conclusion of the timescale of the model. As seen in Figure 5, the ratio [MEK]/[butane] when only OH is considered (lower solid line) is considerably lower at the end of the model than when halogen chemistry is included, even though the simulated OH concentrations are quite high, suggesting that Cl chemistry plays a dominant role in determining the [MEK]/[n-butane] ratios, under the conditions of ozone depletion events. The dotted line showing a model case that includes bromine chemistry (displaced slightly vertically for clarity) demonstrates the negligible effect of Br atom chemistry on this ratio.

[33] While several Arctic ground-level measurements of VOCs have been published [*Ramacher et al.*, 1997; *Ariya et*

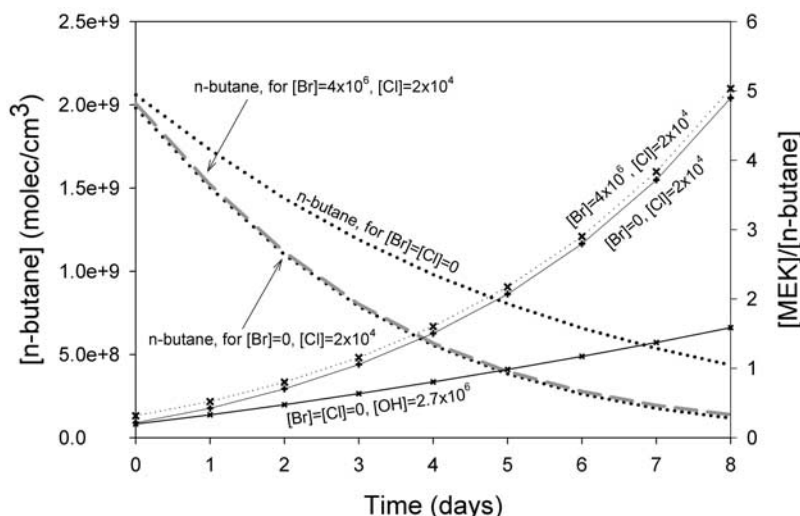


**Figure 5.** Simulated n-butane oxidation by OH or Cl versus time, with indicated average daytime radical concentrations at the completion of the model.

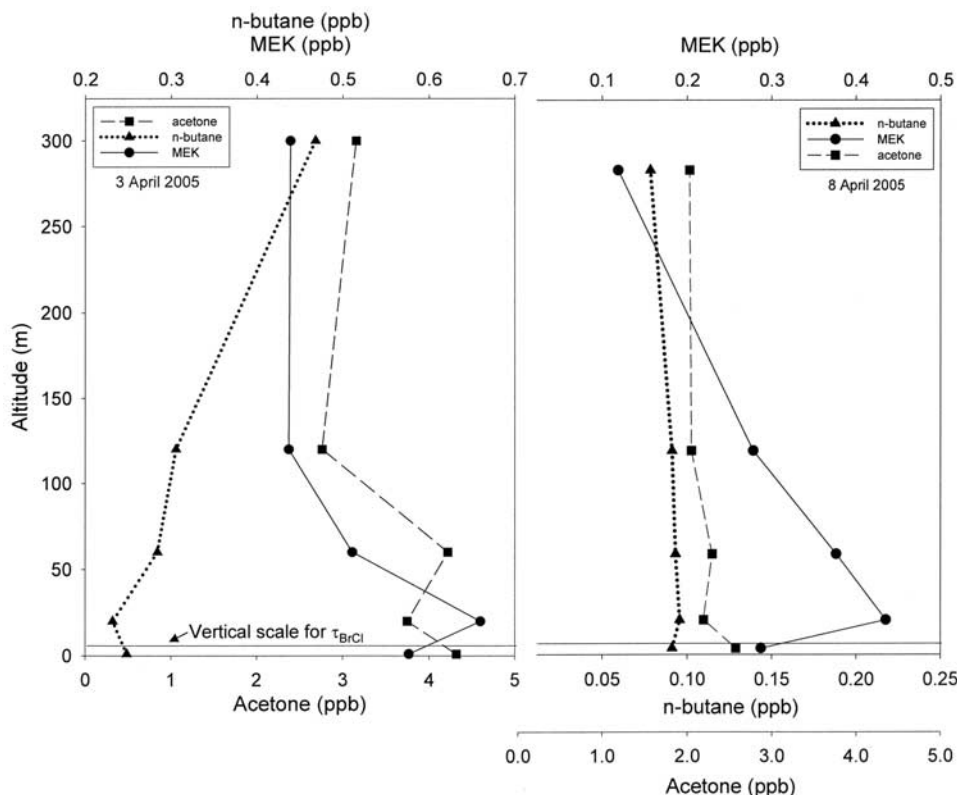


**Figure 6.** Vertical concentration profiles of n-butane, MEK, and acetone obtained during two separate balloon flights during the measurement campaign.

*al.*, 1998; Grannas *et al.*, 2002; Guimbaud *et al.*, 2002; Houdier *et al.*, 2002; Perrier *et al.*, 2002], there is no information to date about the near surface vertical concentration profiles of hydrocarbons, which could provide insight into the vertical scale of the Cl atom chemistry. Figure 6 demonstrates the vertical profiles (mole fraction) for n-butane ( $C_4H_{10}$ ), acetone ( $CH_3C(O)CH_3$ , produced in part from the reaction of Cl with propane [Guimbaud *et al.*, 2002]), and the oxidation product of n-butane, methyl ethyl ketone (MEK), for two separate balloon-based sampler flights, conducted 3 and 8 April 2005.

[34] The VOC data presented in Figure 6 demonstrate the considerable change in concentration over a limited vertical range. N-butane exhibits a very broad range in mole fraction between the two data sets, from less than 100 ppt (on 8 April) to approximately 500 ppt. This range is, however, consistent with previous Arctic n-butane measurements made at Alert, Narwhal, Spitsbergen, and Barrow [Ariya *et al.*, 1998]. Incidences of very low n-butane mole fraction (<0.1 ppb) were also reported by Ariya *et al.* [1998] at the Narwhal ice camp. Light hydrocarbon measurements reported by Jobson *et al.* [1994] indicate a strong seasonal trend in [n-butane], maximizing at 0.62 ppb in winter and minimizing at 0.015 ppb during the summer. It should be noted that during the flight on 8 April, the measurement region was experiencing a broad, near total ozone depletion event, while ozone was only partially depleted ( $\sim 27$  ppb) on 3 April (Figure 2). The concurrent low n-butane and ozone mole fractions recorded on 8 April (and the [MEK]/[butane] ratios presented in Figure 7) are consistent with

enhanced halogen chemistry, believed to play a critical role in the destruction of both species.

[35] The most obvious aspect of the data presented in Figure 6 is that both acetone and MEK are elevated in the lowest 100 m. It has been reported that acetone can be produced within the snowpack, on the basis of gas phase measurements of snowpack interstitial air [Boudries *et al.*, 2002; Dominé and Shepson, 2002; Grannas *et al.*, 2002; Guimbaud *et al.*, 2002]. The long lifetime and thus higher concentrations for acetone would likely lead to a less distinct vertical profile, as observed. For the Arctic at sunrise direct n-butane oxidation is the only known significant source of atmospheric MEK, although there could be some long-range transport of MEK to the region. The acetone measurements on 8 April are consistent with concentrations reported in the literature [Yokouchi *et al.*, 1994; Shepson *et al.*, 1996; Houdier *et al.*, 2002; Grannas *et al.*, 2002; Guimbaud *et al.*, 2002], who report mean acetone mole fractions in the 0.5 to 2 ppb range, but are considerably higher on 8 April.

[36] The OH- and chlorine-induced oxidation product of n-butane (reactions (R14)–(R16)), methyl ethyl ketone (MEK), exhibits a striking vertical concentration profile with a maximum at  $\sim 20$  m, again indicative of the likelihood of oxidative precursors evading from the snowpack in the vicinity of the measurement site. As shown in Figure 7, the [MEK]/[butane] ratio increases by about a factor of 2 descending through the bottom 200 m of the atmosphere, indicating a much greater rate of butane oxidation at the surface. The similar shape in the [MEK]/[butane] ratio plots for both flights suggest that the precursors (e.g., BrCl)

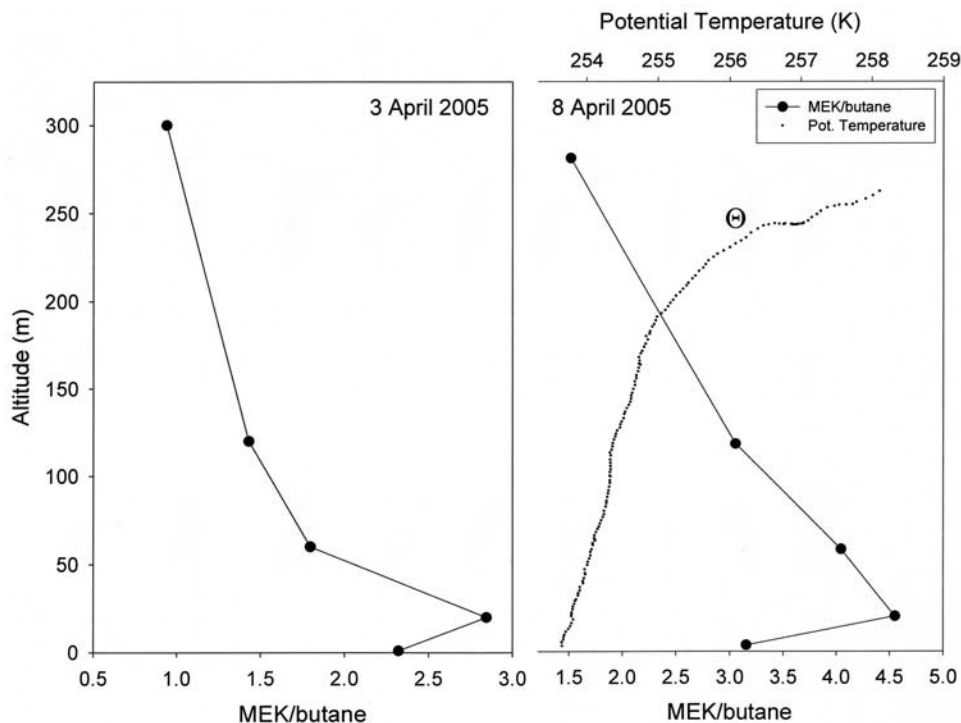


**Figure 7.** [MEK]/[butane] ratio from data presented in Figure 6, including measured potential temperature.

leading to the chemistry responsible for both the destruction of n-butane and the production of MEK are derived from the snowpack. This hypothesis is further substantiated by the meteorological conditions prevailing during the measurements. The dotted plot shown for 8 April in Figure 7 demonstrates the potential temperature data taken directly from the sampling apparatus suspended beneath the balloon (as described in section 2). The positive nature of the slope of the potential temperature profile implies the inherent stability of the atmosphere during the measurements, suggesting that species emitted from the snowpack will mix upward very slowly. The fact that the ratio increases by a factor of 2 descending through the lowest 200 m for 8 April is again consistent with the apparent more active ozone depletion and thus halogen chemistry on that day. A change in [MEK]/[butane] ratio of 2 requires (from equation (3)) a Cl concentration of  $\sim 6.0 \times 10^4$  molecules  $\text{cm}^{-3}$  over a 24 hour timescale for this chemistry to occur, which is consistent with estimated Arctic tropospheric Cl concentrations [Jobson *et al.*, 1994; Boudries and Bottenheim, 2000; Keil and Shepson, 2006].

[37] As discussed earlier, the only significant known sources of reactive halogen atoms that lead to the destruction of Hg and VOCs are  $\text{Br}_2$  and  $\text{BrCl}$ , with  $\text{BrCl}$  being the only known important source of Cl in the Arctic. Given a value for  $J_{\text{BrCl}}$  of  $1.30 \times 10^{-3} \text{ s}^{-1}$  [Madronich and Flocke, 1998] (during midday at Barrow, Alaska), we can also calculate the effective mixing height of  $\text{BrCl}$  in a manner similar to that shown previously for  $\text{Br}_2$  (equation (1)). Using surface-level turbulent eddy diffusivities ( $K_c$ ) ranging from 95 [Guimbaud *et al.*, 2002] to  $700 \text{ cm}^2 \text{ s}^{-1}$  [Lehrer *et al.*, 2004b], the effective mixing height of  $\text{BrCl}$  varies from 2.5 to 10 m, based on a range of  $J$  values from  $6.00 \times 10^{-4}$

to  $1.30 \times 10^{-3} \text{ s}^{-1}$ . The reasonably short calculated vertical distance suggests that halogen atom-induced chemistry would take place over a very limited vertical scale if the halogen atom precursors were indeed produced in the snowpack, which is reasonably consistent with the vertical profile data presented in Figure 6. The slightly broader vertical scale of elevated [MEK]/[butane] ratio may result from diffusion of the VOC reactants from aloft (likely by wind-induced turbulent mixing within the otherwise stable boundary layer) into the lower, chemically depleted region, and diffusion of the products both up and down.

[38] Figure 7 also shows a maximum in the [MEK]/[butane] ratio at  $\sim 20$  m for both flights. Previous work has suggested a variety of mechanisms by which similar components become incorporated into the snowpack. Soluble species such as acetaldehyde ( $\text{CH}_3\text{CHO}$ ) and formaldehyde ( $\text{HCHO}$ ) are believed to undergo adsorptive uptake onto the surface of the snow crystals [Grannas *et al.*, 2002; Perrier *et al.*, 2002; Houdier *et al.*, 2002] during the evening, as the snow surface cools. Such a nighttime surface uptake may explain the MEK data if it is produced in the gas phase from n-butane, but not from oxidation of organic matter in the snowpack, and if the near-surface MEK is lost to the surface by adsorptive uptake. In summary, all of the  $\text{O}_3$ , Hg, and VOC data reported here are consistent with halogen chemistry occurring in the near surface air, implying a surface source for the halogen precursors leading to their destruction.

#### 4. Conclusions

[39] Our results demonstrate that the observed GEM depletion occurred over a limited vertical spatial scale

concurrent with O<sub>3</sub> depletion. The GEM profiles, including the profile on 26 March, are consistent with a model of halogen-induced mercury oxidation taking place within the first ~100 m, followed by deposition of RGM and particulate phase Hg into the snowpack in a manner consistent with Lindberg *et al.* [2001]. The eventual fate of mercury may involve, to some extent, photoinduced reduction and reemission as described by Poulain *et al.* [2004], and as suggested here by the lack of total GEM destruction measured at the lowest altitudes of the profiles, even when O<sub>3</sub> is nearly completely destroyed. At this point, considerable uncertainty lies in the air/snow interface processing of deposited Hg and its rate of emission into the lower atmosphere. The halogen chemistry that consumes O<sub>3</sub>, GEM, and VOCs appears to occur over a small vertical scale, i.e., within a few 10 s of meters from the snowpack. Measurements of n-butane and its oxidation product MEK are consistent with a surface-based source of chlorine precursors. The lifetime of species in the Arctic atmosphere that are consumed mostly by reacting with halogen radicals is likely then determined by the timescale for diffusion into the lowest ~200 m. Given the resulting VOC, O<sub>3</sub>, and GEM vertical profiles, in addition to the relative atmospheric stability during the measurement time, this data set appears consistent with the proposition that the halogen precursors responsible for these chemical mechanisms are most likely emitted from the snowpack. These suggestions could further be corroborated through the measurement of reactants throughout the boundary layer to better understand the timescale of diffusion into the surface layer where the chemistry is likely to occur. In addition, vertical profile data for other reactants (such as propane, which oxidizes to produce acetone, and specific halogen radicals) could provide additional insight into the extent of Cl-induced oxidation at the surface level. Further work is also necessary to remove the uncertainty in the reaction pathways and fate of Arctic GEM to fully understand the impact of halogen chemistry in the lower polar troposphere.

[40] **Acknowledgments.** This work was funded by grant OPP-0325361 of the National Science Foundation. S.M. acknowledges the French Polar Institute (IPEV, grant OOTI 2005-n°440) for financial support. The authors wish to thank Sam Oltmans of the Global Monitoring Division of NOAA for the use of CMDL ozone and radiation data. In addition, we wish to thank Robert Santini and Randy Replogle of the Jonathan Amy Facility for Chemical Instrumentation (JAFCI) at Purdue University for their assistance in the design and construction of the VOC instrumentation and balloon winch used in the project. The authors are also very grateful for the invaluable logistical assistance provided by the personnel of the Barrow Arctic Science Consortium (BASC). This work is part of the international, multidisciplinary Ocean-Atmosphere-Sea Ice-Snowpack (OASIS) Interactions Program.

## References

- Albert, M. R., A. M. Grannas, J. Bottenheim, P. B. Shepson, and F. E. Perron (2002), Processes and properties of snow-air transfer in the high Arctic with application to interstitial ozone at Alert, Canada, *Atmos. Environ.*, *36*, 2779–2787.
- Anlauf, K. G., R. E. Mickle, and N. B. A. Trivett (1994), Measurement of ozone during Polar Sunrise Experiment 1992, *J. Geophys. Res.*, *99*, 25,345–25,353.
- Ariya, P. A., B. T. Jobson, R. Sander, H. Niki, G. W. Harris, J. F. Hopper, and K. G. Anlauf (1998), Measurements of C<sub>2</sub>–C<sub>7</sub> hydrocarbons during the Polar Sunrise Experiment 1994: Further evidence for halogen chemistry in the troposphere, *J. Geophys. Res.*, *103*, 13,169–13,180.
- Ariya, P. A., *et al.* (2004), The Arctic: A sink for mercury, *Tellus, Ser. B*, *56*, 397–403.
- Atkinson, R., D. L. Baulch, R. A. Cox, J. N. Crowley, R. F. Hampson Jr., J. A. Kerr, M. J. Rossi, and J. Troe (2001), Summary of evaluated kinetic and photochemical data for atmospheric chemistry, IUPAC Subcomm. on Gas Kinet. Data Eval. for Atmos. Chem., Research Triangle Park, N. C.
- Banic, C. M., S. T. Beauchamp, R. J. Tordon, W. H. Schroeder, A. Steffen, K. A. Anlauf, and H. K. T. Wong (2003), Vertical distribution of gaseous elemental mercury in Canada, *J. Geophys. Res.*, *108*(D9), 4264, doi:10.1029/2002JD002116.
- Barrie, L. A., J. W. Bottenheim, R. C. Schnell, P. J. Crutzen, and R. A. Rasmussen (1988), Ozone destruction and photochemical reactions at polar sunrise in the lower Arctic troposphere, *Nature*, *334*, 138–141.
- Berg, T., S. Sekkesaeter, E. Steinnes, A. K. Valdal, and G. Wibetoe (2003), Springtime depletion of mercury in the European Arctic as observed at Svalbard, *Sci. Total Environ.*, *304*, 43–51.
- Bottenheim, J. W., A. G. Gallant, and K. A. Brice (1986), Measurements of NO<sub>y</sub> species and O<sub>3</sub> at 82°N latitude, *Geophys. Res. Lett.*, *13*, 113–116.
- Bottenheim, J. W., J. D. Fuentes, D. W. Tarasick, and K. G. Anlauf (2002), Ozone in the Arctic lower troposphere during winter and spring 2000 (ALERT2000), *Atmos. Environ.*, *36*, 2535–2544.
- Boudries, H., and J. W. Bottenheim (2000), Cl and Br atom concentrations during a surface boundary layer ozone depletion event in the Canadian high Arctic, *Geophys. Res. Lett.*, *27*, 517–520.
- Boudries, H., J. W. Bottenheim, C. Guimbaud, A. M. Grannas, P. B. Shepson, S. Houdier, S. Perrier, and F. Domine (2002), Distribution and trends of oxygenated hydrocarbons in the high Arctic derived from measurements in the atmospheric boundary layer and interstitial snow air during the ALERT2000 field campaign, *Atmos. Environ.*, *36*, 2573–2583.
- Calvert, J. G., and S. E. Lindberg (2005), Mechanisms of mercury removal by O<sub>3</sub> and OH in the atmosphere, *Atmos. Environ.*, *39*, 3355–3367.
- Cuevas, C. A., A. Notario, E. Martinez, and J. Albaladejo (2004), A kinetic study of the reaction of Cl with a series of linear and ramified ketones as a function of temperature, *Phys. Chem. Chem. Phys.*, *6*, 2230–2236.
- DeMore, W. B., and K. D. Bayes (1999), Rate constants for the reactions of hydroxyl radical with several alkanes, cycloalkanes, and dimethyl ether, *J. Phys. Chem. A*, *103*, 2649–2654.
- DeMore, W. B., S. P. Sander, D. M. Golden, R. F. Hampson, M. J. Kurylo, C. J. Howard, A. R. Ravishankara, C. E. Kolb, and M. J. Molina (1997), Chemical kinetics and photochemical data for use in stratospheric modeling. Evaluation number 12, *JPL Publication 97-4*, Jet Propul. Lab., Pasadena, Calif.
- Dominé, F., and P. B. Shepson (2002), Air-snow interactions and atmospheric chemistry, *Science*, *297*, 1506–1510.
- Dommergue, A., C. P. Ferrari, P. Gauchard, C. F. Boutron, L. Poissant, M. Pilote, P. Jitaru, and F. C. Adams (2003), The fate of mercury species in a sub-arctic snowpack during snowmelt, *Geophys. Res. Lett.*, *30*(12), 1621, doi:10.1029/2003GL017308.
- Donohoue, D. L., D. Bauer, B. Cossairt, and A. J. Hynes (2006), Temperature and pressure dependent rate coefficients for the reaction of Hg with Br and the reaction of Br with Br: A pulsed laser photolysis-pulsed laser induced fluorescence study, *J. Phys. Chem. A*, *110*, 6623–6632.
- Ebinghaus, R., H. H. Kock, C. Temme, J. W. Einax, A. G. Löwe, A. Richter, J. P. Burrows, and W. H. Schroeder (2002), Antarctic springtime depletion of atmospheric mercury, *Environ. Sci. Technol.*, *36*, 1238–1244.
- Fan, S.-M., and D. J. Jacob (1992), Surface ozone depletion in Arctic spring sustained by bromine reactions on aerosols, *Nature*, *359*, 522–524.
- Foster, K. L., R. A. Plastringe, J. W. Bottenheim, P. B. Shepson, B. J. Finlayson-Pitts, and C. W. Spicer (2001), The role of Br<sub>2</sub> and BrCl in surface ozone destruction at Polar Sunrise, *Science*, *291*, 471–474.
- Gong, S. L., J. L. Walmsley, L. A. Barrie, and J. F. Hopper (1997), Mechanisms for surface ozone depletion and recovery during Polar Sunrise, *Atmos. Environ.*, *31*, 969–981.
- Goodsite, M. E., J. M. C. Plane, and H. Skov (2004), A theoretical study of the oxidation of Hg<sup>0</sup> to HgBr<sub>2</sub> in the troposphere, *Environ. Sci. Technol.*, *38*, 1772–1776.
- Grannas, A. M., *et al.* (2002), A study of photochemical and physical properties affecting carbonyl compounds in the Arctic atmospheric boundary layer, *Atmos. Environ.*, *36*, 2733–2742.
- Guimbaud, C., *et al.* (2002), Snowpack processing of acetaldehyde and acetone in the Arctic atmospheric boundary layer, *Atmos. Environ.*, *36*, 2743–2752.
- Hausmann, M., and U. Platt (1994), Spectroscopic measurement of bromine oxide and ozone in the high Arctic during Polar Sunrise Experiment 1992, *J. Geophys. Res.*, *99*, 25,399–25,413.
- Helmig, D., J. Boulter, D. David, J. W. Birks, N. J. Cullen, K. Steffen, B. J. Johnson, and S. J. Oltmans (2002), Ozone and meteorological boundary-layer conditions at Summit, Greenland, during 3–21 June 2000, *Atmos. Environ.*, *36*, 2595–2608.
- Helmig, D., F. Bocquet, L. Cohen, and S. J. Oltmans (2007), Ozone uptake to the polar snowpack at Summit, Greenland, *Atmos. Environ.*, in press.

- Hönninger, G., and U. Platt (2002), Observations of BrO and its vertical distribution during surface ozone depletion at Alert, *Atmos. Environ.*, *36*, 2481–2489.
- Hönninger, G., H. Leser, O. Sebastián, and U. Platt (2004), Ground-based measurements of halogen oxides at the Hudson Bay by active longpath DOAS and passive MAX-DOAS, *Geophys. Res. Lett.*, *31*, L04111, doi:10.1029/2003GL018982.
- Honrath, R. E., and D. A. Jaffe (1992), The seasonal cycle of nitrogen oxides in the Arctic troposphere at Barrow, Alaska, *J. Geophys. Res.*, *97*, 20,615–20,630.
- Honrath, R. E., M. C. Peterson, S. Guo, J. E. Dibb, P. B. Shepson, and B. Campbell (1999), Evidence of NO<sub>x</sub> production within or upon ice particles in the Greenland snowpack, *Geophys. Res. Lett.*, *26*, 695–698.
- Honrath, R. E., Y. Lu, M. C. Peterson, J. E. Dibb, M. A. Arsenaault, N. J. Cullen, and K. Steffen (2002), Vertical fluxes of NO<sub>x</sub>, HONO, and HNO<sub>3</sub> above the snowpack at Summit, Greenland, *Atmos. Environ.*, *36*, 2629–2640.
- Hopper, J. F., L. A. Barrie, A. Silis, W. Hart, A. J. Gallant, and H. Dryfhout (1998), Ozone and meteorology during the 1994 Polar Sunrise Experiment, *J. Geophys. Res.*, *103*, 1481–1492.
- Houdier, S., S. Perrier, F. Domine, A. Cabanes, L. Legagneux, A. M. Grannas, C. Guimbaud, P. B. Shepson, H. Boudries, and J. W. Bottenheim (2002), Acetaldehyde and acetone in the Arctic snowpack during the ALERT2000 campaign. Snowpack composition, incorporation processes and atmospheric impact, *Atmos. Environ.*, *36*, 2609–2618.
- Impey, G. A., P. B. Shepson, D. R. Hastie, L. A. Barrie, and K. G. Anlauf (1997), Measurements of photolyzable chlorine and bromine during the Polar Sunrise Experiment 1995, *J. Geophys. Res.*, *102*, 16,005–16,010.
- Impey, G. A., C. M. Mihele, K. G. Anlauf, L. A. Barrie, D. R. Hastie, and P. B. Shepson (1999), Measurements of photolyzable halogen compounds and bromine radicals during the Polar Sunrise Experiment 1997, *J. Atmos. Chem.*, *34*, 21–37.
- Jacobi, H.-W., M. M. Frey, M. A. Hutterli, R. C. Bales, O. Schrems, N. J. Cullen, K. Steffen, and C. Koehler (2002), Measurements of hydrogen peroxide and formaldehyde exchange between the atmosphere and surface snow at Summit, Greenland, *Atmos. Environ.*, *36*, 2619–2628.
- Jobson, B. T., H. Niki, Y. Yokouchi, J. Bottenheim, F. Hopper, and R. Leitch (1994), Measurements of C<sub>2</sub>–C<sub>6</sub> hydrocarbons during the Polar Sunrise 1992 Experiment: Evidence for Cl atom and Br atom chemistry, *J. Geophys. Res.*, *99*, 25,355–25,368.
- Jobson, B. T., S. A. McKeen, D. D. Parrish, F. C. Fehsenfeld, D. R. Blake, A. H. Goldstein, S. M. Schlauffer, and J. W. Elkins (1999), Trace gas mixing ratio variability versus lifetime in the troposphere and stratosphere: Observations, *J. Geophys. Res.*, *104*, 16,091–16,113.
- Keil, A. D., and P. B. Shepson (2006), Chlorine and bromine atom ratios in the springtime Arctic troposphere as determined from measurements of halogenated volatile organic compounds, *J. Geophys. Res.*, *111*, D17303, doi:10.1029/2006JD007119.
- Kieser, B. N., J. W. Bottenheim, T. Sideris, and H. Niki (1993), Spring 1989 observations of lower tropospheric chemistry in the Canadian high Arctic, *Atmos. Environ., Part A*, *27*, 2979–2988.
- Lalonde, J. D., A. J. Poulain, and M. Amyot (2002), The role of mercury redox reactions in snow on snow-to-air mercury transfer, *Environ. Sci. Technol.*, *36*, 174–178.
- Langenberg, S., and U. Schurath (1999), Ozone destruction on ice, *Geophys. Res. Lett.*, *26*, 1695–1698.
- Lehrer, E., G. Hönninger, and U. Platt (2004a), The mechanism of halogen liberation in the polar troposphere, *Atmos. Chem. Phys. Disc.*, *4*, 3607–3652.
- Lehrer, E., G. Hönninger, and U. Platt (2004b), A one dimensional model study of the mechanism of halogen liberation and vertical transport in the polar troposphere, *Atmos. Chem. Phys.*, *4*, 2427–2440.
- Lindberg, S. E., A. F. Vette, C. Miles, and F. Schaedlich (2000), Mercury speciation in natural waters: Measurement of dissolved gaseous mercury with a field analyzer, *Biogeochemistry*, *48*, 237–259.
- Lindberg, S. E., S. Brooks, C.-J. Lin, K. Scott, T. Meyers, L. Chambers, M. Landis, and R. Stevens (2001), Formation of reactive gaseous mercury in the Arctic: Evidence of oxidation of Hg-II compounds after Arctic sunrise, *Water Air Soil Pollut.*, *1*, 295–302.
- Lindberg, S. E., S. Brooks, C. Lin, K. J. Scott, M. L. Landis, R. K. Stevens, M. Goodsite, and A. Richter (2002), Dynamic oxidation of gaseous mercury in the Arctic troposphere at Polar Sunrise, *Environ. Sci. Technol.*, *36*, 1245–1256.
- Lu, J. Y., W. H. Schroeder, L. A. Barrie, A. Steffen, H. E. Welch, K. Martin, L. Lockhart, R. V. Hunt, G. Boila, and A. Richter (2001), Magnification of atmospheric mercury deposition to polar regions in springtime: The link to tropospheric ozone depletion chemistry, *Geophys. Res. Lett.*, *28*, 3219–3222.
- Madronich, S., and S. Flocke (1998), The role of solar radiation in atmospheric chemistry, in *Handbook of Environmental Chemistry*, edited by P. Boule, pp. 1–26, Springer, New York.
- Michalowski, B. A., J. S. Francisco, S.-M. Li, L. A. Barrie, J. W. Bottenheim, and P. B. Shepson (2000), A computer model study of multiphase chemistry in the Arctic boundary layer during Polar Sunrise, *J. Geophys. Res.*, *105*, 15,131–15,145.
- Mickle, R. E., J. W. Bottenheim, W. R. Leitch, and W. Evans (1989), Boundary-layer ozone depletion during AGASP-II, *Atmos. Environ.*, *23*, 2443–2449.
- Mickley, L. J., D. J. Jacob, and D. Rind (2001), Uncertainty in preindustrial abundance of tropospheric ozone: Implications for radiative forcing calculations, *J. Geophys. Res.*, *106*, 3389–3399.
- Muthuramu, K., P. B. Shepson, J. W. Bottenheim, B. T. Jobson, H. Niki, and K. G. Anlauf (1994), Relationships between organic nitrates and surface ozone destruction during Polar Sunrise Experiment 1992, *J. Geophys. Res.*, *99*, 25,369–25,378.
- Oltmans, S. J., and W. D. Komhyr (1986), Surface ozone distributions and variations from 1973–1984: Measurements at the NOAA Geophysical Monitoring for Climatic Change Baseline Observatories, *J. Geophys. Res.*, *91*, 5229–5236.
- Perrier, S., S. Houdier, F. Domine, A. Cabanes, L. Legagneux, A. L. Sumner, and P. B. Shepson (2002), Formaldehyde in Arctic snow: Incorporation into ice particles and evolution in the snowpack, *Atmos. Environ.*, *36*, 2695–2705.
- Peterson, M. C., and R. E. Honrath (2001), Observations of rapid photochemical destruction of ozone in snowpack interstitial air, *Geophys. Res. Lett.*, *28*, 511–514.
- Poulain, A. J., J. D. Lalonde, M. Amyot, J. A. Shead, A. Raofie, and P. A. Ariya (2004), Redox transformations of mercury in an Arctic snowpack at springtime, *Atmos. Environ.*, *38*, 6763–6774.
- Pszenny, A. A. P., W. C. Keene, D. J. Jacob, S. Fan, J. R. Maben, M. P. Zetwo, M. Springer-Young, and J. N. Galloway (1993), Evidence of inorganic chlorine gases other than hydrogen chloride in marine surface air, *Geophys. Res. Lett.*, *20*, 699–702.
- Ramacher, B. J., J. Rudolph, and R. Koppmann (1997), Hydrocarbon measurements in the spring Arctic troposphere during the ARCTOC 95 campaign, *Tellus, Ser. B*, *49*, 466–485.
- Ramacher, B. J., J. Rudolph, and R. Koppmann (1999), Hydrocarbon measurements during tropospheric ozone depletion events: Evidence for halogen chemistry, *J. Geophys. Res.*, *104*, 3633–3653.
- Raofie, F., and P. A. Ariya (2003), Kinetics and products study of the reaction of BrO radicals with gaseous mercury, *J. Phys. IV*, *107*, 1119–1121.
- Raofie, F., and P. A. Ariya (2004), Product study of the gas-phase BrO-initiated oxidation of Hg<sup>0</sup>: Evidence for stable Hg<sup>1+</sup> compounds, *Environ. Sci. Technol.*, *38*, 4319–4326.
- Richter, A., F. Wittrock, M. Eisinger, and J. P. Burrows (1998), GOME observations of tropospheric BrO in northern hemispheric spring and summer 1997, *Geophys. Res. Lett.*, *25*, 2683–2686.
- Rudolph, J., R. F. Ban, A. Thompson, K. Anlauf, and J. Bottenheim (1999), Halogen atom concentrations in the Arctic troposphere derived from hydrocarbon measurements: Impact on the budget of formaldehyde, *Geophys. Res. Lett.*, *26*, 2941–2944.
- Russell, J. J., J. A. Seetula, and D. Gutman (1988), Kinetics and thermochemistry of CH<sub>3</sub>, C<sub>2</sub>H<sub>5</sub>, and i-C<sub>3</sub>H<sub>7</sub>: Study of the equilibrium R + HBr → R-H + Br, *J. Am. Chem. Soc.*, *110*, 3092–3099.
- Sander, R., and P. J. Crutzen (1996), Model study indicating halogen activation and ozone destruction in polluted air masses transported to the sea, *J. Geophys. Res.*, *101*, 9121–9138.
- Sander, R., R. Vogt, G. W. Harris, and P. J. Crutzen (1997), Modeling the chemistry of ozone, halogen compounds, and hydrocarbons in the Arctic troposphere during spring, *Tellus, Ser. B*, *49*, 522–532.
- Schroeder, W. H., K. G. Anlauf, L. A. Barrie, J. Y. Lu, A. Steffen, D. R. Schneeberger, and T. Berg (1998), Arctic springtime depletion of mercury, *Nature*, *394*, 331–332.
- Shepson, P. B., A.-P. Sirju, J. F. Hopper, L. A. Barrie, V. Young, H. Niki, and H. Dryfhout (1996), Sources and sinks of carbonyl compounds in the Arctic Ocean boundary layer: Polar Ice Floe Experiment, *J. Geophys. Res.*, *101*, 21,081–21,089.
- Simpson, W. R., L. Alvarez-Aviles, T. A. Douglas, M. Sturm, and F. Domine (2005), Halogens in the coastal snow pack near Barrow, Alaska: Evidence for active bromine air-snow chemistry during springtime, *Geophys. Res. Lett.*, *32*, L04811, doi:10.1029/2004GL021748.
- Slemr, F., B. Ernst-Gunther, R. Ebinghaus, C. Temme, J. Munthe, I. Wangberg, W. Schroeder, A. Steffen, and T. Berg (2003), Worldwide trend of atmospheric mercury since 1977, *Geophys. Res. Lett.*, *30*(10), 1516, doi:10.1029/2003GL016954.
- Spivakovsky, C. M., R. Yevich, J. A. Logan, S. C. Wofsy, M. B. McElroy, and M. J. Prather (1990), Tropospheric OH in a three-dimensional

- chemical tracer model: An assessment based on observations of  $\text{CH}_3\text{CCl}_3$ , *J. Geophys. Res.*, *95*, 18,411–18,471.
- Sproviseri, F., N. Pirrone, M. S. Landis, and R. K. Stevens (2005), Atmospheric mercury behavior at different altitudes at Ny Alesund during Spring 2003, *Atmos. Environ.*, *39*, 7646–7656.
- Steffen, A., W. Schroeder, J. Bottenheim, J. Narayan, and J. Fuentes (2002), Atmospheric mercury concentrations: Measurements and profiles near snow and ice surfaces in the Canadian Arctic during Alert 2000, *Atmos. Environ.*, *36*, 2653–2661.
- Steffen, A., W. Schroeder, R. MacDonald, L. Poissant, and A. Konoplev (2005), Mercury in the Arctic atmosphere: An analysis of eight years of measurements of GEM at Alert (Canada) and a comparison with observations at Amderma (Russia) and Kuujjuarapik (Canada), *Sci. Total Environ.*, *342*, 185–198.
- Sumner, A. L., and P. B. Shepson (1999), Snowpack production of formaldehyde and its effect on the Arctic troposphere, *Nature*, *398*, 230–233.
- Swanson, A. L., N. J. Blake, J. E. Dibb, M. R. Albert, D. R. Blake, and F. S. Rowland (2002), Photochemically induced production of  $\text{CH}_3\text{Br}$ ,  $\text{CH}_3\text{I}$ ,  $\text{C}_2\text{H}_5\text{I}$ , ethene, and propene within surface snow at Summit, Greenland, *Atmos. Environ.*, *36*, 2671–2682.
- Tang, T., and J. C. McConnell (1996), Autocatalytic release of bromine from Arctic snow pack during Polar Sunrise, *Geophys. Res. Lett.*, *23*, 2633–2636.
- Thompson, A. M. (1995), Measuring and modeling the tropospheric hydroxyl radical (OH), *J. Atmos. Sci.*, *52*, 3315–3327.
- Tossell, J. A. (2003), Calculation of the energetics for oxidation of gas-phase elemental Hg by Br and BrO, *J. Phys. Chem. A*, *107*, 7804–7808.
- Tyndall, G. S., J. J. Orlando, T. J. Wallington, M. Dill, and E. W. Kaiser (1997), Kinetics and mechanisms of the reactions of chlorine atoms with ethane, propane, and n-butane, *Int. J. Chem. Kinet.*, *29*, 43–55.
- Vogt, R., P. J. Crutzen, and R. Sander (1996), A mechanism for halogen release from sea salt aerosol in the remote marine boundary layer, *Nature*, *383*, 327–330.
- Wesely, M. L., and B. B. Hicks (2000), A review of the current status of knowledge on dry deposition, *Atmos. Environ.*, *34*, 2261–2282.
- Yokouchi, Y., H. Akimoto, L. A. Barrie, J. W. Bottenheim, K. Anlauf, and B. T. Jobson (1994), Serial gas chromatographic/mass spectrometric measurements of some volatile organic compounds in the Arctic atmosphere during the 1992 Polar Sunrise Experiment, *J. Geophys. Res.*, *99*, 25,379–25,389.
- Zhou, X., H. J. Beine, R. E. Honrath, J. D. Fuentes, W. Simpson, and P. B. Shepson (2001), Snowpack photochemical production of HONO: A major source of OH in the Arctic boundary layer in springtime, *Geophys. Res. Lett.*, *28*, 4087–4090.
- 
- J. W. Bottenheim, J. Deary, and A. Steffen, Science and Technology Branch, Environment Canada, Toronto, ON, Canada M3H 5T4.
- A. E. Cavender, A. D. Keil, P. B. Shepson, and P. J. Tackett, Department of Chemistry, Purdue University, West Lafayette, IN 47907, USA. (pshepson@purdue.edu)
- C. Doerge, Jonathan Amy Facility for Chemical Instrumentation, Purdue University, West Lafayette, IN 47907, USA.
- S. Morin, Laboratoire de Glaciologie et Géophysique de l'Environnement, 54 rue Molière, F-38400 Saint Martin d'Hères, France.